



ELSEVIER

Available online at www.sciencedirect.com

SCIENCE @ DIRECT®

Physica C 392–396 (2003) 259–262

PHYSICA C

www.elsevier.com/locate/physc

X-ray absorption and resonant photoemission spectroscopy of ZrB_2

S. Tsuda ^{a,*}, R. Eguchi ^a, A. Kosuge ^a, T. Yokoya ^a, A. Fukushima ^a, S. Shin ^{a,b},
A. Chainani ^c, S. Otani ^d, Y. Takano ^d, K. Togano ^d, H. Kito ^e

^a Institute for Solid State Physics (ISSP), University of Tokyo, 5-1-5 Kashiwanoha, Kashiwa, Chiba 277-8581, Japan

^b RIKEN, 1-1-1 Kouto, Mizuki-cho, Sayo, Hyogo 679-5148, Japan

^c IPR, B-15-17/P, Sector-25, GIDC Electronic Estate, Gandhinagar 382 044, Gujarat, India

^d NIMS, 1-2-1 Sengen, Tsukuba, Ibaraki 305-0047, Japan

^e AIST, 1-1-1 Umezono, Tsukuba, Ibaraki 305-8568, Japan

Received 13 November 2002; accepted 31 January 2003

Abstract

We have performed X-ray absorption and valence band photoemission spectroscopy on ZrB_2 , which has the same AlB_2 structure of MgB_2 , to study the electronic structure. From X-ray absorption spectra near the B 1s–2p threshold, we found a small absorption edge at 188.23 eV with a negligible angular dependence upto 190 eV photon energy. This indicates that B 2p partial density of states near the Fermi level (E_F) is three dimensional, in sharp contrast to that of MgB_2 . Resonant photoemission study across the B 1s–2p threshold was found to be difficult due to a large contribution of Auger electrons. On the other hand, resonant photoemission across the Zr 3p–4d threshold does show small change in intensity within 4 eV of E_F . This indicates that the occupied states near E_F have substantial Zr 4d character. These observations are in relatively good agreement with band structure calculations.

© 2003 Elsevier B.V. All rights reserved.

PACS: 78.70.Dm; 79.60.-i; 71.20.Lp

Keywords: MgB_2 related compounds; Photoemission

1. Introduction

Diborides (MB_2 , M = metals) have been studied for a long time due to the industrially important properties such as high melting point, hardness, chemical stability and so on. After the unexpected discovery of high temperature superconductivity in

MgB_2 [1], diborides have attracted renewed attention because of motivations like obtaining higher transition temperatures (T_c) in the related materials and understanding the mechanism of the superconductivity in MgB_2 by comparing the electronic structures [2].

Among the diborides, ZrB_2 was reported to be a superconductor [3], though later a severe sample dependence ($T_c = 0$ –5.5 K) of the superconductivity was found. For the electronic structure, long time ago, Ihara et al. have performed X-ray

* Corresponding author. Tel./fax: +81-4-7136-3545.

E-mail address: tsuda@issp.u-tokyo.ac.jp (S. Tsuda).

photoemission study and concluded the importance of the graphitic boron network of the electronic structure with the help of band calculations [4]. However, while comparison of the calculated electronic structure with that of MgB_2 has been reported recently, detailed experimental studies are not reported.

In this paper, we present X-ray absorption (XA) and resonant photoemission (RPE) spectroscopy of ZrB_2 high quality single crystals. We discuss the overall electronic structure: the occupied and unoccupied states, the contribution of boron and/or zirconium atoms, and the dimensionality of boron network.

2. Experimental

The ZrB_2 single crystals (typical size of $5 \times 5 \times 3 \text{ mm}^3$) were synthesized by the floating zone method as described in detail in Ref. [5]. XA and RPE measurements were performed at BL19B of Photon Factory, High Energy Accelerator Research Organization, Japan. We checked the orientation of all the samples using Laue diffraction pattern, and measured with two configurations as shown in the inset of Fig. 1; (a) the incident photon direction is parallel to the c -axis with the electronic field parallel to the a -axis or (b) the incident photon direction is 60° with respect to the c -axis with the electronic field in the ac plane. We call those configurations as (a) $k\parallel c$ and (b) $k\parallel a$ for convenience. All the sample surfaces in this study were prepared by scraping with a diamond filer inside ultra-high vacuum at room temperature and all the measurements were done at room temperature. The base pressure of the measurement chamber was about 8×10^{-10} Torr. The photon energies were in the B 1s–2p threshold region (180–220 eV) and the Zr 3p–4d threshold region (325–355 eV). XA spectra in the total electron yield (TEY) mode were recorded by measuring sample current. We measured XA spectra by the total fluorescence yield (TFY) mode using an X-ray ultraviolet (XUV) silicon photodiode with an energy resolution of about 300 meV, which is known to be more bulk sensitive than the TEY mode, and we obtained the same results as the TEY mode. In

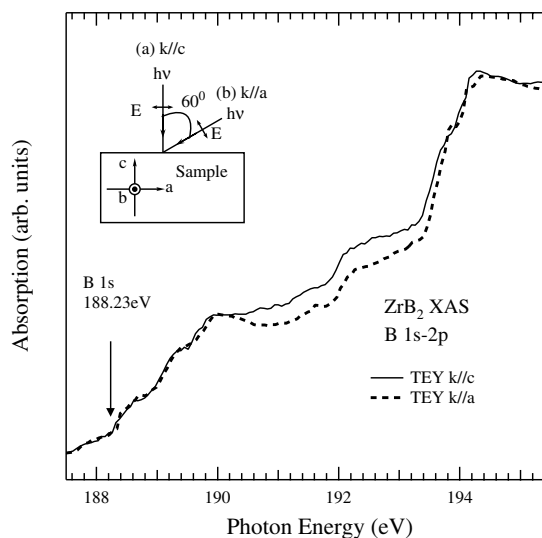


Fig. 1. B 1s–2p XA spectra. The solid line shows the $k\parallel c$ spectrum and the broken line shows the $k\parallel a$ spectrum. The inset shows the ' $k\parallel c$ ' and ' $k\parallel a$ ' configurations.

this paper, we show only the results of the TEY mode because of its better signal to noise ratio. PE measurements were performed using a VG CLAM4 photoelectron energy analyzer with a total energy resolution of about 300 meV. The photon energy was calibrated using the Au 4f core level and using the second order light. When the signal of the second order light was too weak, we made calibration using the Au 4f core level energy position. The accuracy of the photon energy was better than 100 meV.

3. Results and discussion

Fig. 1 shows the XA spectra of ZrB_2 across the B 1s–2p threshold region, which reflect the B 2p partial unoccupied density of states (DOS). The horizontal axis shows the incident photon energy. The solid line shows the $k\parallel c$ spectrum and the broken line shows the $k\parallel a$ spectrum. Apart from photon energy scale of 190–194 eV, these two spectra are very similar to each other. The difference of the spectra between the $k\parallel c$ and $k\parallel a$ configurations reflects the symmetry of the electronic

states. Since the incident photon is linearly polarized, the electrons dispersing in the ab plane are easily excited in $k\parallel c$ configuration and those dispersing along the c -axis are easily excited in $k\parallel a$. Considering these, we can infer two different symmetries for B 2p unoccupied states. The $k\parallel c$ spectrum should correspond to B 2p $_{\sigma}$ states and the $k\parallel a$ spectrum should correspond to B 2p $_{\pi}$ states, whose assigns as well as spectral shapes show quite good agreement with the band calculation [6]. Vertical arrow indicates the energy position of the B 1s core level at 188.23 eV, which was determined by PE measurement. The absorption edge position is almost the same as that of the B 1s core level. This result indicates, as expected for a normal metal, that the exciton effect is not so important. The fact that the spectra near the absorption edge accord with each other indicates B 2p electronic states near the E_F are three dimensional, in contrast to MgB $_2$ case [7], where they are two dimensional. Following the XA study, we measured PE spectra in this energy region, and observed a strong peak originated from Auger electrons. PE spectra of MgB $_2$ polycrystalline samples measured in the same energy region also show a strong Auger peak. These results indicates that B 1s–2p resonant photoemission spectroscopy is not suited to study the electronic structure of the diborides due to a large contribution of the Auger process.

Fig. 2 shows the XA spectra in the Zr 3p–4d threshold region. The solid line shows the $k\parallel c$ spectrum and the broken line shows the $k\parallel a$ spectrum. Different from the B 1s–2p threshold region, the XA spectra in this energy region do not reflect the partial DOS of Zr 4d but the local electronic states connected with multipole correlation effect [8]. The Zr 4d electronic states are three dimensional since there is no difference between the spectra of the two configurations.

Fig. 3 shows the photon energy dependence of the PE spectra across the Zr 3p–4d threshold region. In Fig. 3, curve (a) shows a off-resonance spectrum and curve (b) and (c) show on-resonance spectra. We observed a clear Fermi edge and three features around 3, 6, and 11 eV binding energies (inset). The spectral shape is nearly the same as the XPS result of Ihara et al. [5]. The most conspicu-

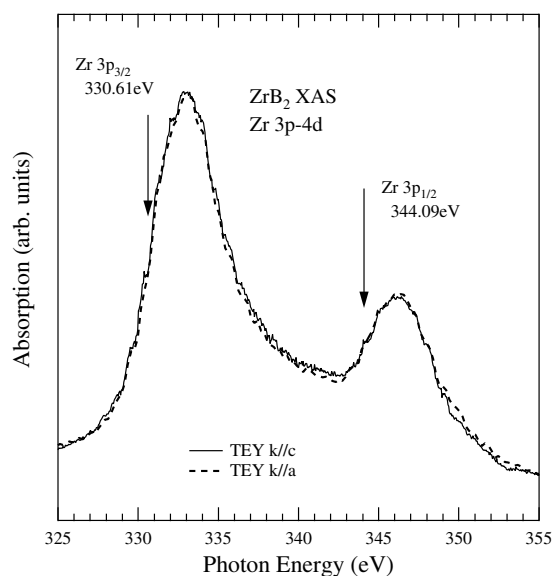


Fig. 2. Zr 3p–4d XA spectra. The solid line shows the $k\parallel c$ spectrum and the broken line shows the $k\parallel a$ spectrum.

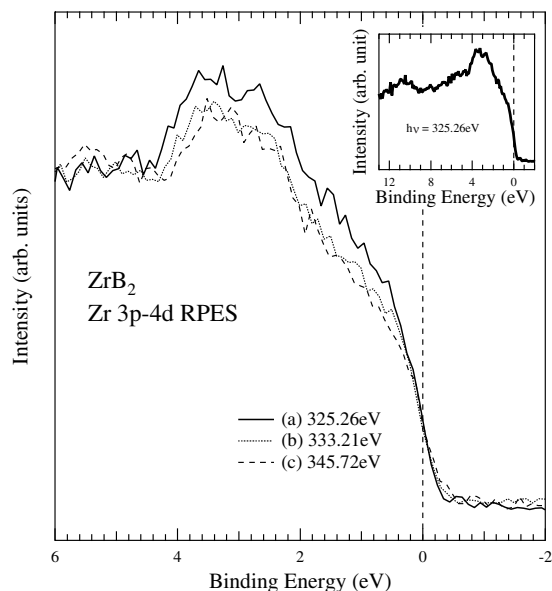


Fig. 3. The photon energy dependence of PE spectra in the Zr 3p–4d region. From 0 to 4 eV binding energy, we observe anti-resonance effect. The inset shows the valence band spectrum in the wide energy region, which has three components around 3, 6, and 11 eV binding energies.

ous difference between the off- and on-resonance spectra is the intensity reduction within 4 eV

binding energy of E_F , where the PE intensity is slightly suppressed in the spectra obtained at 333.21 and 345.72 eV. This result indicates that ZrB_2 shows an anti-resonant behavior and that Zr4d electrons substantial around that binding energy region, which is consistent with the calculated band structures [6].

In summary, we measured XA spectra and PE spectra of ZrB_2 in the B 1s–2p threshold region and the Zr 3p–4d threshold region. The XA spectra and its polarization dependence on the B 1s–2p threshold region show that unoccupied states near E_F consist of both B2p $_{\sigma}$ and B2p $_{\pi}$ states, providing evidence for three dimensional states near E_F . In the B 1s–2p threshold region, since we observed strong Auger signals on the PE spectra in the ZrB_2 and MgB_2 , it was hard to identify the resonance effect. PE spectra of Zr 3p–4d threshold region show anti-resonance effect, which indicates that the Zr4d contribution dominates within 4 eV binding energy of E_F . The experimentally deter-

mined electronic structure of ZrB_2 is consistent with band structure calculations.

References

- [1] J. Nagamatsu, N. Nakagawa, T. Muranaka, Y. Zentani, J. Akimitsu, *Nature* 410 (2001) 63.
- [2] As a review C. Bueza, T. Yamashita, *Supercond. Sci. Technol.* 14 (2001) R115.
- [3] V.A. Gasparov, N.S. Sidorov, I.I. Zverkova, M.P. Kulakov, *JETP Lett.* 73 (2001) 532.
- [4] H. Ihara, M. Hirabayashi, H. Nakagawa, *Phys. Rev. B* 16 (1977) 726.
- [5] S. Otani, Y. Ishizawa, *J. Cryst. Growth* 165 (1996) 319; S. Otani, M.M. Korsukova, T. Mitsunashi, *J. Cryst. Growth* 186 (1998) 582.
- [6] H. Rosner, J.M. An, W.E. Pickett, S.-L. Drechsler, *Phys. Rev. B* 66 (2002) 024521.
- [7] S. Schuppler, E. Pellegrin, N. Nucker, T. Mizokawa, M. Merz, D.A. Arena, J. Dvřak, Y.U. Idzerda, D.-J. Haung, C.-F. Cheng, K.-P. Bohnen, R. Heid, P. Schweiss, Th. Wolf, *cond-mat/0205230*, 2002.
- [8] F.M.F. de Groot, Ph.D. thesis, 1991.